Effects of Confinement on the Thermodynamics of a Collapsing Heteropolymer: An Off-Lattice Wang−Landau Monte Carlo Simulation Study

Yelena Sliozberg and Cameron F. Abrams*

Department of Chemical and Biological Engineering, Drexel University, 3141 Chestnut St., Philadelphia, Pennsylvania 19104

Received March 2, 2005; Revised Manuscript Received April 15, 2005

ABSTRACT: We present an analysis of the thermodynamics of the coil-to-globule transition of a bead−spring heteropolymer in selective solvent conditions in confined geometries. We have used the continuous-space version of the Wang−Landau Monte Carlo simulation algorithm. Generally, decreasing volume of confinement stabilizes the compact state, reflected directly by an increase in the transition temperature, in agreement with previous theoretical pictures. We propose a new scaling relationship for the shift in the transition temperature in which the changes in latent heat and latent entropies upon confinement scale with the confining geometry size with slightly different scaling exponents. The model agrees with the simulation data well and slightly outperforms simpler scaling models used in the past. Details of the algorithm, including novel trial moves, are presented and discussed. In particular, we find it useful to use so-called "partial molecular dynamics" trial moves.

I. Introduction

Understanding protein folding is one of the most important goals of modern science. In recent years, there has been a strong focus on understanding the role of "confinement" and "crowding" on protein folding because the natural cytoplasmic environments in which proteins fold are crowded with other proteins, protein complexes, lipid bilayer structures, and more, which can both confound and assist a newly transcribed polypeptide's search for its native conformation. Generically, forcing any polypeptide into a confined space must affect its thermodynamic behavior as compared to its behavior in dilute solution. Quantifying the degree to which this generic effect is important for any particular protein and environment may one day prove crucial in engineering protein production pathways. As such, there has been a significant amount of research in recent years aimed understanding how confinement in general affects protein thermodynamics.

Experimental results show that confinement enhances the thermal stability of proteins in the native state. Eggers and Valentine observed a 25−30 °C increase in the native-to-coil melting temperature of α-lactalbumin using a sol−gel entrapment system.[1] In a separate study, these authors also noted similar stabilization of encapsulated apomyoglobin.[2] Bollis et al. observed a similar stabilization effect for four single domain proteins: titin 127 and bacterial, yeast, and human frataxins, wherein the largest increase in melting temperature, about 5 °C in polyacrylamide gel, was observed for the least stable of the examined proteins, yeast frataxin.[3] Ravindra et al. observed a roughly 30 °C stabilization against temperature-induced unfolding of RNase A when encapsulated in a mesoporous silica using calorimetry.[4] Particular attention has been paid to the *E. coli*−chaperonin complex GroEL/GroES, a 21-subunit complex with a ∼85 000 Å^3 cavity within which protein folding is catalyzed.[5−7] Brinker and co-workers, using a rapid biotin−streptavidin-based inhibition of chaperonin function, showed that mere confinement of a range of synthetic polypeptides in the GroEL cage significantly enhances folding throughput comparing with spontaneous, unassisted folding.[7,8]

Partial explanations of this behavior from theory hold that the primary mechanism is a destabilization of the unfolded state due to confining geometry's restriction on the number of accessible "open" conformations. The consequent reduction in conformational entropy of the unfolded state shifts the equilibrium population distribution toward the native state. Using a statistical thermodynamic model, Minton estimates the effect of excluded volume due to macromolecular crowding or confining media as an increase in the unfolding temperature by 5−20 °C.[9,10] Similarly, Zhou and Dill showed that mere mechanical confinement in a small inert cage would stabilize a protein against reversible unfolding by excluding some expanded conformations of the unfolded chain.[11,12] These authors predicted an increase in the melting temperature of 31 °C for α-lactalbumin, in agreement with measurements of Eggers and Valentine.

Several studies using direct simulation have corroborated and expanded the theoretical picture of confinement's effect on protein stability. Ping et al. performed standard Boltzmann Monte Carlo of HP lattice proteins in order to investigate two kinds of confinement: inside a rigid box and tethered to a solid surface.[13,14] These authors found that confinement indeed stabilizes folded conformations relative to unfolded, and they found that melting temperatures increase with decreasing confinement dimension. Liu and Haynes found increased stability of a lattice HP protein adsorbed on a 2D surface when laterally confined.[15] Klimov et al. studied the effect of confinement in an inert spherical cavity on thermodynamic behavior of a small (16-mer) off-lattice coarse-grained model protein using Langevin dynamics.[16] They observed that

* Corresponding author. E-mail: cfa22@drexel.edu.

10.1021/ma050443t CCC: $30.25
Published on Web 05/18/2005

even modest confinement increases the stability of native states, where "modest" is defined as cavity radii larger than about twice the radius of gyration of the native peptide. Takagi et al., also using Langevin dynamics, expanded on the work of Klimov et al. by considering several larger coarse-grained model proteins in inert cylindrical cavities. These authors found support for a simple scaling relationship of the transition, or "melting," temperature, T_m, and the confining cavity size L of the form $\Delta T_m \sim (R_0/L)^\nu$, where $\nu \approx 3$ and R_0 is the characteristic size of the polypeptide.[17] This scaling, however, was only valid for relatively "strong" confinement, where "strong" is defined as cavity sizes smaller than about twice the radius of gyration of the native peptide. Baumketner et al. considered the effects of confinement in a sphere on the collapse and folding transitions of a small α/β polypeptide using straightforward molecular dynamics of a minimalist model, showing the collapse transition temperature increased with decreasing confining sphere size for spheres with diameters less than roughly twice the size of the native, folded structure.[18] More recently, Cheung et al. used Langevin dynamics/replica exchange simulations to show that a globular protein's melting temperature scales with the volume fraction of crowding agents with an exponent of 1.8 and, more interestingly, that the kinetics of folding in a crowded enviroment have a strong similarity to the kinetics of folding in a single confining cavity.[19]

The off-lattice studies[16,17,19] are intriguing because they reveal that "modest" confinement is important but that simple scaling is apparently only valid at "strong" confinement. A more complete theoretical picture is therefore still wanting. Furthermore, these off-lattice studies also made use of Go-like Hamiltonians, which encode a preference for the native state into the potential energy terms explicitly, rather than allowing unbiased atomic-scale interactions to determine the folded state. This artificially stabilizes the ground state in a way difficult to decouple from the apparent additional stabilization granted by confinining the peptides. Finally, it should be appreciated that the simulation results described above are synthesized from many individual simulations at various temperatures to reconstruct the full thermodynamic behavior over a temperature range of interest. If it is true that confinement acts to reduce the conformational freedom of open states, then what is actually being probed is the effect of confinement on the density of states of the polypeptide, $g(U)$, where U is potential energy, which is itself independent of temperature. If $g(U)$ is known, thermodynamic quantities can be calculated for any temperature. It is therefore desirable to show directly that confinement changes the density of states. A relatively new direct simulation method, due to Wang and Landau,[20,21] allows calculation of $g(U)$ in a single simulation. The so-called Wang−Landau density of states Monte Carlo method has been used by Rathore and de Pablo to study the thermodynamics of a simple, off-lattice polypeptide in dilute solution conditions.[22,23]

The main focus of our work is to study the effect of mechanical confinement in a spherical cavity on the thermodynamics of a simple bead−spring heteropolymer using the Wang−Landau MC method. We have chosen a model heteropolymer which is designed to form a particular microphase-separated core−shell collapsed structure, rather than a particular protein, to emphasize the best possible performance of a generic scaling relation. We are particularly interested in how confinement can stabilize collapsed or partially states vs open states, manifest as an increase in the transition temperature with increasing confinement, and how we can use the unique insights offered by the Wang−Landau technique to develop a better scaling theory for the melting temperature. Of more technical interest, we also discuss how best to adapt the Wang−Landau method for use in continuous-space simulations of single macromolecules in confinement. Our paper is organized as follows. In section II, our simulation techniques are discussed, including the model heteropolymer, system initialization, and details of the Wang−Landau technique developed for our study are presented. In section III, we discuss our results, dealing both with (i) heteropolymer thermodynamics through a simple model of the stabilization mechanism and (ii) adapting the Wang−Landau method for use in off-lattice macromolecular simulation. We then conclude in section IV.

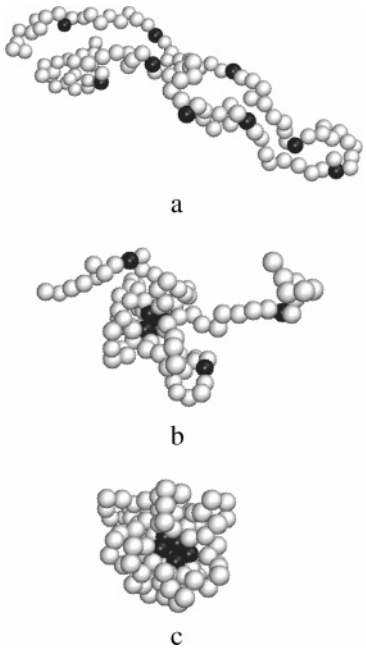

Figure 1. Representative snapshots of the A_9B heteropolymer: (a) an "open" conformation; (b) a "partially collapsed" conformation; (c) a "fully collapsed" conformation.

II. Simulation Techniques

A. The Model Heteropolymer. A three-dimensional system composed of a single chain of a generic multiblock copolymer is encapsulated in a spherical pore of variable size with repulsive walls. The chain has length $N = 109$ monomers, represented by the palindromic sequence $(A_9B)_{10}A_9$. Type "A" monomers may be thought of as hydrophilic and type B as hydrophobic. A snapshot of such a heteropolymer in an open conformation appears in Figure 1a. Particle interactions are pairwise additive and depend on the particle type and existence of chemical bonds between the monomers. A reduced unit system is adopted for convenient expression of parameters: length is measured in units of the particle diameter σ and energy in units of ϵ. The unit of temperature is ϵ/k_B, where k_B is Boltzmann's constant. The total potential energy U of a system configuration

$\mathbf{r}^N$ is given by a sum of Lennard-Jones, bonded, and wall interactions:

$$U(\mathbf{r}^N) = \sum_i \sum_{j>i} U_{LJ}(r_{ij}) + \sum_{kl} U_{FENE/LJ}(r_{kl}) + \sum_i U_w(r_i) \tag{1}$$

where the double sum in the first term involves only nonbonded pairs of particles, while the summation in the second term involves only bonded pairs of particles. The third term accounts for repulsive interactions with the wall of the confining sphere. Generally, the pair interaction between topologically nonconnected particles is described by the standard Lennard-Jones pair potential:

$$U_{LJ}^{\alpha\beta}(r) = \begin{cases} 4n\left[\left(\frac{1}{r}\right)^{12} - \left(\frac{1}{r}\right)^{6} - \left(\frac{1}{r_c^{\alpha\beta}}\right)^{12} + \left(\frac{1}{r_c^{\alpha\beta}}\right)^{6}\right] & r < r_c^{\alpha\beta} \\ 0 & r \geq r_c^{\alpha\beta} \end{cases} \tag{2}$$

where $\alpha\beta \in$ (AA, BB, AB). BB pairs interact with an full Lennard-Jones potential with an attractive well; AB and AA pairs interact with a fully repulsive truncated Lennard-Jones potential. For the fully repulsive interactions, we choose $r_c^{AA} = r_c^{AB} = 2^{1/6}$, yielding so-called Weeks−Chandler−Andersen excluded-volume potential,[24] denoted U_{WCA}. For attractive interactions, we choose $r_c = 4.0$. To ensure phase separation, we choose the factor n equal to 10.0 for attractive interactions, while it is equal to unity for any repulsive interactions. For modest temperatures near unity, we know these strong attractive interactions drive a phase separation to a collapsed, core−shell structure, as shown in Figure 1c; this is discussed in detail in section III.

Topologically bound monomers interact according to the standard FENE/Lennard-Jones bonded potential, $U_{FENE/LJ}$:[25]

$$U_{FENE/LJ}(r) = U_{WCA}(r) + U_{FENE}(r) \tag{3}$$

where

$$U_{FENE}(r) = -\frac{a}{2}R_0^2 \ln\left[1 - \left(\frac{r}{R_0}\right)^2\right] \tag{4}$$

We choose standard parameter values of $R_0 = 1.5$ and $a = 30.0$.[26]

Repulsive interactions between the spherical wall and any particle are given by a 10−4 Lennard-Jones potential, U_w:[27]

$$U_w(r) = \begin{cases} 2\pi\left(\frac{2}{5}r^{-10} - r^{-4} + \frac{3}{5}\right) & r < r_c \\ r < r_c & r \geq r_c \end{cases} \tag{5}$$

where r is the distance between the wall and particle and r_c is equal to 1.0. We have studied confining radii of size $R = 5$, 7, 10, 20 and bulk (i.e., "infinite" radius).

B. System Initialization. The initial configuration of a heteropolymer is constructed as a random walk of N beads in 3D continuous space with a step equal to 0.97 (where $U_{FENE/LJ}(r)$ is minimal). To guarantee separation between particles, a two-stage preequilibrium "warm-up" simulation is performed to introduce excluded volume gently and to place the heteropolymer in a spherical pore. In stage 1, all pairwise nonbonded forces during the warm-up are derived from the fully repulsive WCA potential (i.e., no attraction), capped at a value of 1.963. The stage 1 simulation consists of 50 000 time steps of length of 0.01 and employs the dissipative particle dynamics (DPD) thermostat,[28,29] with a friction of 0.5 and a temperature of 1.0. Bound monomers interact according to the standard FENE/Lennard-Jones bonded potential, $U_{FENE/LJ}$. In stage 2, to insert the chain into a spherical pore of a certain size, we create a pore, centered on the molecule center of mass, with diameter equal to the maximum end-to-end distance. We then perform constant temperature molecular dynamics simulation by reducing the sphere radius by 0.01σ each time step until the desired pore size is reached. This second molecular dynamics warm-up employs U_{WCA}, $U_{FENE/LJ}$ for bound monomers, and the repulsive wall potential U_w. Both warm-up stages are performed using the standard velocity-Verlet integrator.[30]

C. Wang−Landau Monte Carlo Simulation of Off-Lattice Heteropolymers in Confinement. The algorithm of Wang and Landau method computes the density of states, $g(U)$, in an iterative fashion.[20,21] Briefly, we consider a finite domain of potential energy, $U_{low} < U < U_{high}$, divided into a finite number of bins of uniform width ΔU. In the course of the simulation, we keep track of two histograms: (a) the number of times each bin is visited, denoted $H(U)$, and (b) the density of states value of each bin, stored as $\ln g(U)$. To begin a simulation, all bins are initialized such that $H(U) = 0$ and $\ln g(U) = 0$. Then a random walk in energy space is initiated by attempting trial moves that change the system potential energy. A move taking the system from bin U_1 to U_2 is accepted according to the probability

$$p_{acc}(U_1 \rightarrow U_2) = \min\left[\frac{g(U_1)}{g(U_2)}, 1\right] \tag{6}$$

A move is rejected outright if $U_2 < U_{low}$ or $U_2 > U_{high}$. After a move, regardless of whether it is accepted or rejected, the histograms are updated according to $H(U) \leftarrow H(U) + 1$ and $\ln g \leftarrow \ln g + \ln f$, where f is a scale factor initially set at 1.064. This random walk simulation is continued until the histogram $H(U)$ is "sufficiently flat". We explored several flatness criteria of various severities and settled on the convention used by Shell et al., namely, that every bin in H has at least 20 hits.[31] At this point, H is rezeroed, $\ln g$ is maintained, and f is reduced according to $f \leftarrow \sqrt{f}$. Iterations in this fashion are chained together until $\ln f < 10^{-8}$, at which time $g(U)$ is taken to be the final density of states.

To determine the appropriate energy range, we conducted Langevin dynamics simulations at various temperatures between $T = 0.5$ and 4.0, beginning from open conformations, and noted the values of U accessed. We require a range from $U_{low} = 1950$ to $U_{high} = 2450$ to observe our chain in all relevant conformations (from open chain to a single-core globule). We divide the energy range into bins of size $\Delta U = 0.1$. This is a smaller bin size than that used by Rathore,[22] but we found that this small bin size results in acceptance of a larger number possible conformations and should consequently lead to a more accurate density of states. We performed five independent runs for each pore size to improve the statistics.

Table 1. Trial Move Weights

move	weight (%) bulk	weight (%) confined
rotational		
crankshaft	13.33	8.33
simple hinge	13.33	8.33
compound hinge	13.33	8.33
global rotation		8.33
translational		29.17
partial MD	60.00	37.50

The energy distribution function at a particular temperature, $P(U)$, can be calculated by

$$P(U_i) \equiv P_i = \frac{g(U_i)e^{-\beta U_i}}{\sum_k g(U_k)e^{-\beta U_k}} \tag{7}$$

where the summation is over all energy bins. We can calculate thermodynamic quantities such as internal energy and specific heat:

$$\langle U(T)\rangle = \sum_i U_i P_i \tag{8}$$

$$C(T) = \frac{\partial\langle U(T)\rangle}{\partial T} = \frac{\langle U^2\rangle_T - \langle U\rangle_T^2}{T^2} \tag{9}$$

It should be mentioned that, without a reference state for which $g(U)$ is known independently, this algorithm only provides $g(U)$ to within an undetermined multiplicative constant. This constant bears no relevance in the computed thermodynamic quantities listed above, including the melting temperature, because it divides out of the probability distribution (eq 7). It is, however, not strictly allowed that we quantitatively compare absolute $g(U)$'s from the simulations among the various values of confining radius.

D. Off-Lattice Trial Moves. One challenge in conducting Wang−Landau simulations for continuous space systems is developing a suitable library of trial moves. We use a mixture of moves including translation of center of mass, rotation of chain subsections around various axes defined by the chain geometry, and short NVE molecular dynamics trajectories. In detail, the trial moves employed are as follows, and their weights are reported in Table 1. Generally speaking, we found it useful to use a combination of global moves (concerted displacements of large segments of the chain or the entire chain itself) and local moves (displacements of small segments).

1. Translation. The center of mass of the molecule is shifted by a random vector $(\delta x,\delta y,\delta z)$, where each displacement is chosen randomly and uniformly between 0.1 and r_c. Clearly, this trial move is only employed for runs in the confining sphere and not in the bulk simulations for which there is no way for translation to produce a new value of U.

2. Global Rotation. A global coordinate system is centered on the molecule center of mass. The entire molecule is rotated by a randomly chosen angle between $-\pi$ and π around the z-axis, then by another angle, its cosine chosen between -1 and 1 around the y-axis, and yet a third time around the z-axis with an angle chosen between $-\pi$ and π. As with translation, this move is only applied for runs in the confining sphere.

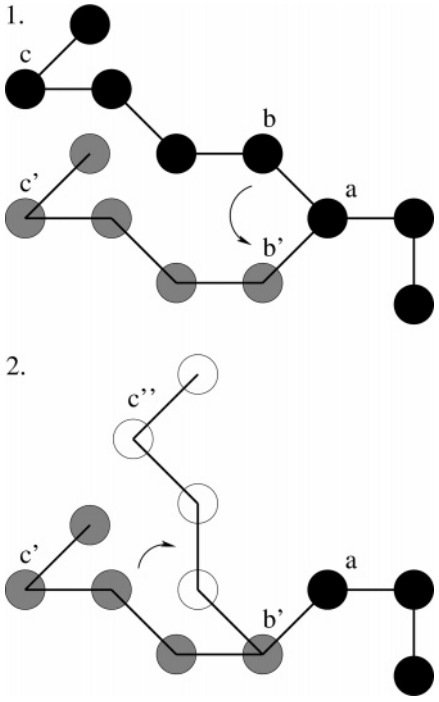

Figure 2. Schematic representation of the compound hinge trial move. Step 1 involves a hinge which swings the bond between "a" and "b"; step 2 swings the chain segment between "b" and "c" as a rigid body.

3. Compound Hinge. We employ an off-lattice version of the traditional lattice hinge move, with an important generalization. Roughly speaking, a hinge move requires a defined subchain to be rotated through space as a rigid body with reference to a single monomer (the "hinge point"), while the remainder of the chain beyond the subchain is translated as a rigid body without rotation to maintain connectivity. In effect, this means that three intramolecular angles are potentially altered; hence, we term this a "compound" hinge and depict it schematically in Figure 2. The details of the compound hinge are as follows. A hinge point monomer is selected at random from internal monomers and designated "a". One of the two neighbors of "a" is chosen randomly, denoted "b", and it is then placed at a random polar angle θ and azimuthal position ϕ, both chosen uniformly, at a fixed distance from "a". (Strictly speaking, ϕ is chosen randomly from $-\pi < \phi < \pi$, and cos θ between $-1 <$ cos $\theta < 1$, to ensure a uniform probability density on a surface of a sphere.) All monomers beyond "b" on the other side of "a" are simply shifted to maintain connectivity (step 1 in Figure 2). At this point, we term this move a "simple" hinge because only two intramolecular angles have been altered. A third monomer, "c", is chosen randomly such that "b" is between "a" and "c". Again, a random angular orientation of "c" relative to "b" at fixed distance is chosen uniformly from the surface of a sphere, and all monomers between "b" and "c" are rotated as one rigid body. Monomers beyond "c" are then shifted to maintain connectivity (step 2 in Figure 2). Hence, the angles at monomers "a", "b", and "c" are changed. Because all monomers and angles are chosen randomly, no balance criterion is violated. If monomer "c" happens to be a chain end, then this becomes a simple hinge move.

4. Crankshaft. An off-lattice version of the traditional lattice crankshaft move is also employed. Here, two monomers separated by at least one monomer along the

chain are chosen and designated a and b. The vector $\mathbf{r}_{ab}$ forms the axis around which monomers between a and b are rotated as a single rigid body by a random angle between 0 and 2π.

5. NVE Molecular Dynamics. While the moves listed above produce both large and small conformational changes, they are insufficient in allowing the system to visit compact configurations in reasonable time. As can be appreciated from Figure 1c, the low-energy conformations our molecule adopts have a relatively densely packed core of B-type monomers. For this reason, it is advantageous to include a trial move which allows collective rearrangement of a large number of monomers. Following the example of Rathore and de Pablo,[22] we therefore incorporate short NVE molecular dynamics trajectories in our library of trial moves.

The use of NVE MD as a trial move within an otherwise standard Boltzmann Monte Carlo simulation has acquired the name "hybrid Monte Carlo".[32] For an NVE MD trial move to satisfy detailed balance, the acceptance probability applied to other trial moves (eq 6) must be modified to

$$p_{\mathrm{acc}}(U_1 \rightarrow U_2) = \min\left[\exp(-\beta\Delta K)\frac{g(U_1)}{g(U_2)}, 1\right] \quad (10)$$

The Boltzmann factor involving the change in kinetic energy, $\Delta K \equiv K_2 - K_1$, arises due to the a priori probabilities of (a) finding the system configuration with kinetic energy K_1 prior to attempting the forward move and (b) finding the system with kinetic energy K_2 prior to attempting the hypothetical reverse move. It is important to note, however, that temperature is not an inherent thermodynamic variable in the Wang−Landau method, yet the MD trial move introduces it in two places: (1) the temperature characterizing the Boltzmann distribution of velocities assigned to the particles to initialize the MD trial move, which we denote T_{MD} ($K_1 = {}^3/_2 N k_{\mathrm{B}} T_{\mathrm{MD}}$), and (2) the temperature in the Boltzmann factor in the acceptance criterion, which we denote T_{B} ($\beta = 1/k_{\mathrm{B}}T_{\mathrm{B}}$). In traditional hybrid MC at constant T, these two temperatures are identical; yet this is not a requirement here. Both of these temperatures are essentially tuning parameters for the random walk in U-space. Nevertheless, all the results discussed here, except in section III.C.1, are performed with $T_{\mathrm{B}} = T_{\mathrm{MD}}$. Section III.C.1 is devoted to a discussion of why this is also a sensible choice for flat-histogram MC methods.

For each global MD move, we randomly select number of MD steps between 1 and 30 and T_{MD} between 0.1 and 3.0 for bulk and between 1.0 and 4.0 for confined runs. Higher values for T_{MD} help in sampling the high-energy regime and with overcoming local minima in any energy regime. Lower values for T_{MD} ensure MD trial moves work in the low-energy regime, favoring collapse of the chain. (These values were arrived at by trial and error; confined runs were slower to converge if the maximum temperature was set at 3.0, for example.) Velocity components are randomly selected for the chosen segment to achieve the selected temperature while constraining the total momentum to zero. Molecular dynamics integration is performed with the standard velocity Verlet algorithm with a time step equal to 0.01.

Another important distinction between our NVE MD trial moves and those typically used in hybrid Boltzmann MC is that we only apply the MD integration to a randomly selected subset of monomers while others are held fixed. The "MD-active" segment is chosen by randomly selecting two monomers, a and b, and requiring that all monomers between a and b are MD-active.

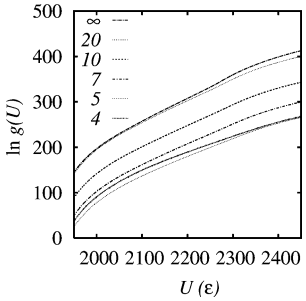

Figure 3. Natural log of the density of states vs total potential energy for different pore sizes.

The strategy behind these "partial" MD trial moves is to allow collective rearrangement on a variety of length scales throughout the simulation. Allowing all monomers to be MD-active for such a large molecule resulted in large fluctations in kinetic energy which often lowered the acceptance rate of MD trial moves to unacceptably low levels. We are allowed to use such moves here because we are effectively tuning the masses of our monomers to make the MD moves more efficient (infinite mass means a monomer does not move), and because masses are not part of the total potential energy (eq 1), no balance criterion is violated. We do not systematically compare the use of "partial" MD to "total" MD trial moves in this work, but our anecdotal observations so far are that their use greatly speeds up convergence in simulations of bulk chains or chains in large pores.

E. Clustering Analysis. During the simulation, we measure cluster size distributions in each energy bin to characterize the conformational states accessed. A cluster is composed of one or more hydrophobes, and if two hydrophobes are separated by less 1.5, they belong to the same cluster. Cluster size is denoted m, and the number of clusters of size m is denoted $n(m)$. Our heteropolymer has 10 hydrophobic beads, so the fully open chain would possess $n = 10$ clusters of size $m = 1$. Likewise, the fully collapsed chain would possess $n = 1$ cluster of size $m = 10$. The clustering analysis is helpful for visualization of a macrostate, corresponding to each energy bin, as an average of microscopically different partially collapsed chains.

III. Results and Discussion

A. Simulation Results. In Figure 3, we show the logarithm of densities-of-state, ln $g(U)$, for different confinement radii, R, and for bulk as a function of total potential energy. These are "raw" simulation results in that no shifting or scaling for reasons of comparison have been made. Each curve is the average of five independently calculated densities-of-state. As discussed previously, we are not strictly allowed to compare the absolute magnitudes of one $g(U)$ to another. However, because each simulation ran for the same number of iterations, we can infer that the higher $g(U)$'s, corresponding to larger R, required many more histogram hits than did the lower $g(U)$'s, corresponding to lower R, to achieve flatness. This is an indirect and slightly imprecise measure of the degree to which confinement reduces $g(U)$. Thus, from Figure 3 we infer that the number of accessible states in the high-energy regime

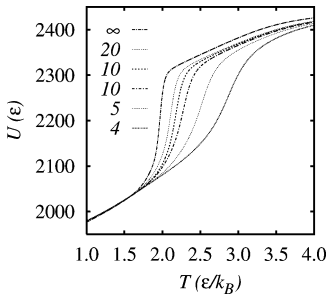

Figure 4. Internal energy vs temperature for different pore sizes.

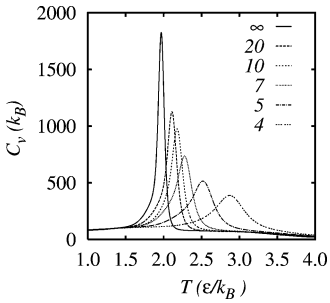

Figure 5. Heat capacity vs temperature for different pore sizes.

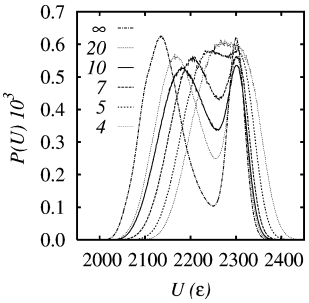

Figure 6. Probability distributions (eq 7) at respective melting temperatures for various pore sizes.

decreases with decreasing pore radius because confinement reduces the number of possible conformations of the open chain. Some expanded conformations of the unfolded chain cannot exist in the confined space.[11]

Fortunately, the $g(U)$ relationships give a direct and unambiguous view of the thermodynamics of our confined heteropolymers. That the heteropolymer undergoes a first-order "melting" transition in bulk can easily be seen from the internal energy, $\langle U(T)\rangle$, shown in Figure 4. The melting temperature, T_m, is identifiable where $\langle U\rangle$ undegoes a sharp jump; for bulk, $T_m^b = 1.96$. For the confined heteropolymers, T_m is seen generally to increase as R decreases, although it is somewhat hard to pinpoint a value for T_m for the lowest R due to the rather shallow nature of the jump. It is also possible to ascribe T_m as the temperature at which there is a peak in the heat capacity, $C(T)$ (eq 9), as depicted in Figure 5. We instead followed the original method of Wang and Landau,[20,21] choosing to ascribe T_m to that temperature at which the two peaks in the probability distribution are of equal height, meaning the most probable microstate in both states have the same probability. Sweeping T in increments of 0.001 from 1.0 to 4.0, we were able to extract $T_m(R)$ from the probability distributions. The probability distributions at the various T_m for each R are plotted in Figure 6, and values for T_m are reported in Table 2. We see that $T_m(R)$ increases as

Table 2. Thermodynamic Properties of the Model Heteropolymer Confined in Spherical Pores of Various Sizes, R^a

R	T_m	ΔU	ΔS
4	2.93	40.0	13.6
5	2.56	63.0	24.6
7	2.29	93.0	40.5
10	2.18	120.0	54.9
20	2.11	137.0	65.0
∞	1.96	165.0	84.2

[a] All values shown are in reduced Lennard-Jones units.

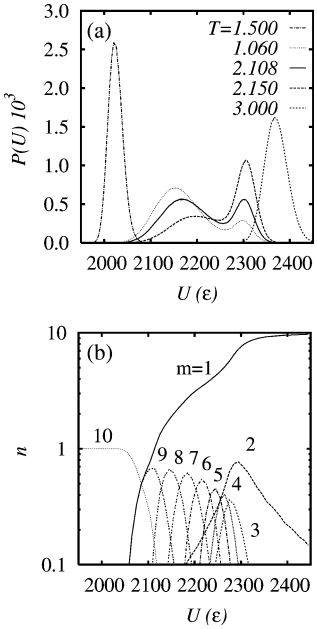

Figure 7. (a) Normalized probability distributions for various temperatures for the case of confinement at $R = 20$. (b) Cluster size distributions as functions of potential energy for $R = 20$; each curve labeled m corresponds to clusters of m hydrophobes, and the y-axis measures the number of clusters, n.

R decreases, indicating that confinement seems to stabilize the low-energy state.

The transition detected in $\langle U\rangle$ is the melting of a compact, core−shell conformation (e.g., Figure 1c) to form an open conformation (e.g., Figure 1a). This is apparent not only from snapshots but also from the clustering analysis. As an example, we consider the case for confinement at $R = 20$. Probability distributions of potential energy for various temperatures are shown in Figure 7a and clearly show the first-order nature of the transition. Below this, in Figure 7b, we show the cluster size distributions as a function of potential energy. We see that, at low energies, the states are mostly comprised of conformations with a large cluster of size eight or higher with the balance made up by single clusters, while at high energies, the states are mostly comprised of conformations of many single hydrophobes. At the lowest energies, we observe conformations with a single cluster of 10 hydrophobes, while at the highest energies, we observe conformations of 10 free hydrophobes. Interestingly, the transition state, identifiable from the probability distribution as the minimum between the two peaks at a temperature of about 2.1, corresponds to conformations with exactly five free hydrophobes.

B. A Simple Thermodynamic Scaling Model for the Shift in the Melting Temperature. The natural log of the density of states is the entropy of the chain

for constant energy according to our adopted reduced unit system:

$$S(U) = k_B T \ln g(U) \tag{11}$$

At an equilibrium between two phases, the free energy of the two phases is equal. Hence

$$\Delta U = T_m \Delta S \tag{12}$$

where ΔU is the change in internal energy upon "melting" (a "latent heat"), ΔS is the corresponding change in entropy (a "latent entropy"), and T_m is the transition, or "melting", temperature. From here, it is straightforward algebra to show change in melting temperature upon confinement is given by

$$\frac{\Delta T_m}{T_m^b} = \frac{\dfrac{\Delta U}{\Delta U^b}}{\dfrac{\Delta S}{\Delta S^b}} - 1 \tag{13}$$

where the superscript "b" denotes the cases for bulk (i.e., no confinement).

With densities of state in hand, we can now address how the latent heat and latent entropy individually depend on the size of the confining sphere. We first note that there is some minimal radius, denoted R_{min}, below which it is impossible to observe a first-order transition. This trend is apparent from the probability distributions in Figure 6: as R decreases, the two distinct peaks merge. Second, we require that, as $R \to \infty$, $\Delta U(R) \to \Delta U^b$ and $\Delta S(R) \to \Delta S^b$. With the properties in mind, we now suppose that, in dimensionless forms, these latent quantities can be expressed as

$$\frac{\Delta U(R)}{\Delta U^b} = \left(1 - \frac{R_{min}}{R}\right)^p \tag{14}$$

$$\frac{\Delta S(R)}{\Delta S^b} = \left(1 - \frac{R_{min}}{R}\right)^q \tag{15}$$

where p and q are positive scaling exponents. Combining this relations, we obtain

$$\frac{\Delta T_m}{T_m^b} = \left(1 - \frac{R_{min}}{R}\right)^\gamma - 1 \tag{16}$$

where $\gamma = p - q$.

By allowing R_{min} and γ to vary, we fit the relation in eq 16 to our simulation data for $\Delta T_m/T_m^b$ and obtained $R_{min} = 2.923$ and $\gamma = -0.306$. This value of R_{min} is close to the mean radius of gyration of the collapsed state, which is about 3. We then used the resulting value of R_{min} in fits of the relations 14 and 15 to obtain $p = 1.060$ and $q = 1.368$. The simulation data and fits for ΔU and ΔS are shown in Figure 8a. In Figure 8b, we plot our scaled shift in melting temperature, with the fit model of eq 16.

First, both the simulation and the model predict that confinement increases the melting temperature, so long as there is a first-order transition to observe. Furthermore, the model states that the melting temperature increases with reduction of the pore size for any $R > R_{min}$ if $\gamma < 0$ or $q > p$. This means that in order for this stabilization to occur the latent entropy must decrease

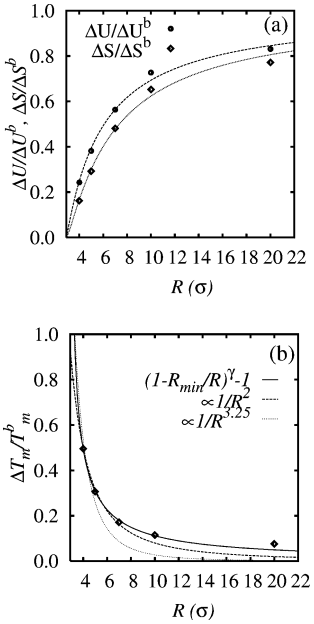

Figure 8. Increase in thermal stability of collapsed states with increasing confinement. (a) Scaled latent heat, ΔU, and latent entropy, ΔS, vs pore size, R. Curves are fits to eqs 14 and 15 with $p = 1.060$, $q = 1.368$, and $R_{min} = 2.923$. (b) Relative shift in melting temperature upon confinement, $\Delta T_m(R)/T_m$, as a function of the pore size. Solid curve is eq 16 with the scaling exponents noted. Dashed curves show scaling relationships with a single exponent of 2 and 3.25, respectively.

with R faster than does the latent heat. In other words, stabilization upon confinement is guaranteed if entropy rather than energy is more sensitive to the confinement volume. In contrast, in the case of positive γ ($p > q$), for $R > R_{min}$, the shift in T_m upon confinement is always negative. This reveals a possible route to using confinement to destabilize folded proteins: the cavity must be designed in such a way that the latent heat is more sensitive to cavity size than is the latent entropy. We might speculate that such a cavity would have a certain density of reactive sites on its inner walls which interact favorably with parts of a protein which are normally buried when it is folded. If the energy of the open state is lowered by interaction with the walls, then we might expect the latent heat to be sensitive to the cavity size by means of the internal surface area. Entropy is generally sensitive to the volume of the cavity, so a cavity that destabilizes folded proteins would be unlikely to be a perfect sphere with smooth walls. We defer exploration of confinement-induced destabilization to a later work.

We now consider whether our form gives a better fit to the simulation data that previous scaling relationships. Also shown in Figure 8b are curves corresponding to simple scaling relationships of the form

$$\frac{\Delta T_m}{T_m^b} \sim R^{-\nu} \tag{17}$$

with ν values of 2 and 3.25,[17] with proportionality constants extracted from fits, for comparison. Our model outperforms both simple scaling laws, especially for large degrees of confinement, where "large" is defined as confining sphere radii almost 10 times as large as the radius of gyration of the collapsed state, R_{min}.

A word of caution is warranted at this point. Our simulations were performed for a single chain length,

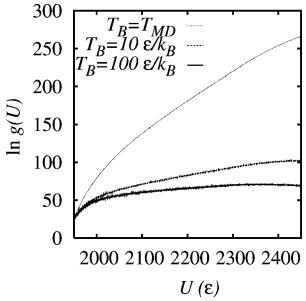

Figure 9. Density of states for different value of T_B from a single simulation with confinement at $R = 5$; $1 < T_{MD} < 4$.

topology (number of hydrophobes), and Hamiltonian, so it is premature to state that we have discovered a "new" scaling behavior for the thermodynamics of intramolecular self-assembly (i.e., "collapse" and "folding") in confined geometries. However, because the Wang−Landau method gives us a detailed view of the thermodynamics, we are able to delineate the effect of confinement on both latent heat and latent entropy, which is difficult if not impossible using other direct simulation techniques so far considered.

C. On the Trial Moves for Off-Lattice Wang−Landau MC of Linear Polymers. *1. The Two Temperatures for NVE MD Trial Moves.* Consider an NVE MD trial move launched from a high-energy bin. The trajectory will likely result in a decrease in U and an increase in K, making ΔK a large positive quantity. The Boltzmann factor in the acceptance criterion (eq 10) will likely prevent the acceptance of such a move. In effect, a low T_B makes the Boltzmann factor powerful in restricting the acceptance of MD trial moves. Conversely, making T_B effectively infinite removes the kinetic Boltzmann factor. This however can lead the system too rapidly to the low-U side of the energy range before the high-U side can be adequately explored using the other moves. Figure 9 shows an example of simulation for one run with $R = 5$ using two high values $T_B = 10$ and $T_B = 100$ and a case of $T_B = T_{MD}$ which we employ for our calculation. Fast propagation in direction of low energy causes unsufficient sampling of high-energy states for high T_B, which our mild flatness criterion for H gives large reduction of visited states. We can estimate propagation speed of simulation by comparing total number of hits for the first iteration of Wang−Landau random walk. The total number of hits for $T_B = T_{MD}$ is $\approx 12.5 \times 10^6$, while for $T_B = 10$, the total number of hits is 5.4×10^6, and for $T_B = 100$ this sinks to 3.9×10^6. Clearly, increasing T_B results in a less efficient random walk over energy space for a given flatness criterion, although it increases the acceptance rate of MD trial moves. While it might be possible to mitigate this effect by making the flatness criterion for H more severe, requiring stricter flatness in H can make the simulation enormously expensive, negating any benefit to be had by increasing acceptance of MD trial moves.

It appears that it is advantageous to make sure that at least some of the MD trial moves are rejected due to an excessive increase in kinetic energy. This degree of rejection is partially tuned by T_B. It seems that value of $\beta\Delta K$ has to be in order of unity to accept reasonable number of fluctuations in kinetic energy, which help promote our chain to the low-energy regime slow enough to count large number of accessible conformations. This effect is obtained by keeping the equality $T_B = T_{MD}$ because fluctuations in kinetic energy in the microcanonical ensemble are proportional to temperature. We have therefore chosen $T_B = T_{MD}$ for all our MD trial moves in production simulations.

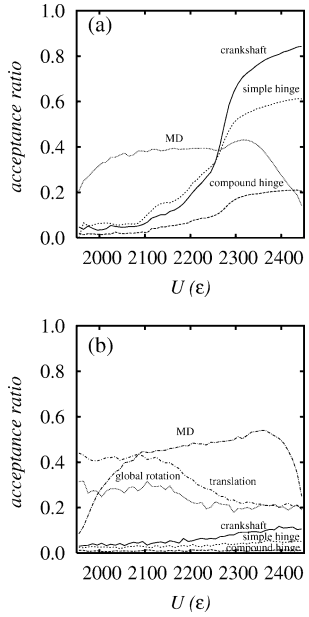

Figure 10. Acceptance ratios vs potential energy for the various trial moves: (a) bulk; (b) confined at $R = 5$.

D. Acceptance Ratios. In Figure 10, we show acceptance ratios for the various trial moves as functions of potential energy of the originating state for any move. Figure 10a shows the acceptance ratios for the bulk simulations, while Figure 10b shows them for the case of confinement at $R = 5$. We observe a good rate of acceptance of the MD moves, about 40%, over a broad span of the energy domain for both bulk and confined simulations. Clearly, MD moves are quite valuable to this method and are relatively more important for strongly confined heteropolymers as opposed to more weakly confined heteropolymers. Also, the bulk simulations benefit greatly from the conformational moves (crankshafts and hinges) only at relatively high energies for which the conformations are predominantly open, as one would expect. For confined simulations, we see that global rotations and translations are crucially important, while they are by construction not needed in the bulk runs. Also in the confined runs, the conformation shifting moves are almost unimportant. It seems that NVE MD, global rotation, and global translation are most important in covering potential energy space, though we noticed that completely neglecting the conformational moves in the bulk runs results in much slower convergence. The relative dominance of MD trial moves suggests the possibility that Wang−Landau Monte Carlo can be performed with only MD trial moves. We are currently exploring this possibility; if shown feasible, it would greatly expand the number of systems to which the Wang−Landau method could be applied, including dense macromolecular systems with explicit solvent.

IV. Conclusions

The Wang−Landau method of direct density-of-states calculation has been used for off-lattice simulation of mechanical confinement of a generic multiblock copoly-

mer undergoing a first-order collapse transition. We have developed a suitable library of trial moves, including a "partial NVE MD" move, which have been shown useful for both free and confined bead−spring heteropolymers. Using this technique, we have quantified the increase in thermal stability of a collapsed globular state in a spherical confining geometry, measured as an increase in melting temperature with decreasing radius of the confining sphere. We showed that a simple scaling relationship that allows the change in latent energy of the transition to scale independently of the change in latent entropy with the radius results in a better fit to the simulation data, compared to simpler scaling relationships considered previously. This indicates a new direction in pursuing a theoretical understanding of both the thermodynamics and kinetics of confined proteins. Moreover, our work supports the use of flat-histogram Monte Carlo methods to study heteropolymer (i.e., protein) thermodynamics in various settings.

Acknowledgment. The authors are grateful to N.-K. Lee for useful insights. This work was partially supported by the NSF through DMR-0427643.

References and Notes

(1) Eggers, D. K.; Valentine, J. S. *Protein Sci.* **2000**, *10*, 250−261.
(2) Eggers, D. K.; Valentine, J. S. *J. Mol. Biol.* **2001**, *314*, 911−922.
(3) Bolis, D.; Politou, A. S.; Kelly, G.; Pastore, A.; Temussi, P. A. *J. Mol. Biol.* **2004**, *336*, 203−212.
(4) Ravindra, R.; Zhao, S.; Gies, H.; Winter, R. *J. Am. Chem. Soc.* **2004**, *126*, 12224−12225.
(5) Sigler, P. B.; Xu, Z.; Rye, H. S.; Burston, S. G.; Fenton, W. A.; Horwich, A. L. *Annu. Rev. Biochem.* **1998**, *67*, 581−608.
(6) Ellis, R. J.; Hartl, F. U. *Curr. Opin. Struct. Biol.* **1999**, *9*, 102−110.
(7) Ellis, R. J. *Curr. Biol.* **2001**, *11*, R1038−R1040.
(8) Brinker, A.; Pfeifer, G.; Kerner, M. J.; Naylor, D. J.; Hartl, F. U.; Hayer-Hartl, M. *Cell* **2001**, *107*, 223−233.
(9) Minton, A. P. *Biophys. J.* **2000**, *78*, 101−109.
(10) Minton, A. P. *J. Biol. Chem.* **2001**, *276*, 10577−10580.
(11) Zhou, H. X.; Dill, K. A. *Biochemistry* **2001**, *40*, 11289−11293.
(12) Zhou, H. X. *J. Mol. Recognit.* **2004**, *17*, 368−375.
(13) Ping, G.; Yuan, J. M.; Vallieres, M.; Dong, H.; Sun, Z.; Wei, Y.; Li, F. Y.; Lin, S. H. *J. Chem. Phys.* **2003**, *118*, 8042−8048.
(14) Ping, G.; Yuan, J. M.; Sun, Z.; Wei, Y. *J. Mol. Recognit.* **2004**, *17*, 433−440.
(15) Liu, S. M.; Haynes, C. A. *J. Colloid Interface Sci.* **2005**, *282*, 283−292.
(16) Klimov, D. K.; Newfield, D.; Thirumalai, D. *Proc. Natl. Acad. Sci. U.S.A.* **2002**, *99*, 8019−8024.
(17) Takagi, F.; Koga, N.; Takada, S. *Proc. Natl. Acad. Sci. U.S.A.* **2003**, *100*, 11367−11372.
(18) Baumketner, A.; Jewett, A.; Shea, J. E. *J. Mol. Biol.* **2003**, *332*, 701−713.
(19) Cheung, M. S.; Klimov, D.; Thirumalai, D. *Proc. Natl. Acad. Sci. U.S.A.* **2005**, *102*, 4753−4758.
(20) Wang, F.; Landau, D. P. *Phys. Rev. Lett.* **2001**, *86*, 2050.
(21) Wang, F.; Landau, D. P. *Phys. Rev. E* **2001**, *64*, 056101.
(22) Rathore, N.; Knotts IV, T. A.; de Pablo, J. J. *J. Chem. Phys.* **2003**, *118*, 4285−4290.
(23) Rathore, N.; Yan, Q.; de Pablo, J. J. *J. Chem. Phys.* **2004**, *120*, 5781−5788.
(24) Weeks, J. D.; Chandler, D.; Andersen, H. C. *J. Chem. Phys.* **1971**, *54*, 5237−5247.
(25) Bishop, M.; Kalos, M. H.; Frisch, H. L. *J. Chem. Phys.* **1979**, *70*, 1299−1304.
(26) Kremer, K.; Grest, G. S. *J. Chem. Phys.* **1990**, *92*, 5057−5086.
(27) Abrams, C. F.; Kremer, K. *J. Chem. Phys.* **2001**, *115*, 2776−2785.
(28) Soddemann, T.; Dünweg, B.; Kremer, K. *Phys. Rev. E* **2003**, *68*, 046702.
(29) Nikunen, P.; Karttunen, M.; Vattulainen, I. *Comput. Phys. Commun.* **2003**, *153*, 407−423.
(30) Swope, W. C.; Andersen, H. C.; Berens, P. H.; Wilson, K. R. *J. Chem. Phys.* **1982**, *76*, 637−649.
(31) Shell, M. S.; Debenedetti, P. G.; Panagiotopoulos, A. Z. *Phys. Rev. E* **2002**, *66*, 056703-1−056703-9.
(32) Mehlig, B.; Heermann, D. W.; Forrest, B. M. *Phys. Rev. B* **1992**, *45*, 679−685.

MA050443T